34th Annual International Conference of the IEEE EMBS
San Diego, California USA, 28 August - 1 September, 2012

In vitro characterization of an aortic bioprosthetic valve using Doppler echocardiography and qualitative flow visualization

Kiran Dellimore, Iain Kemp, Reynaldo Rodriguez and Cornie Scheffer, *Member, IEEE*

***Abstract*—A 19 mm diameter prototype bioprosthetic valve mounted in a cardiac pulse duplicator was characterized using Doppler echocardiography and qualitative flow visualization at a heart rate of 72 bpm. Analysis of the flow visualization images revealed that the prototype and control valve leaflets open symmetrically but close asymmetrically. The asymmetry in the closing of the valves is likely due to the large pressure gradients across the valves and may have implications for the long term mechanical failure of the valves. The relatively high peak systolic velocity of 309.9 cm/s, which was measured in the prototype 19 mm valve, can be attributed to the small valve diameter and the high cardiac output used in the current study.**

I. INTRODUCTION

Aortic valve stenosis caused by progressive calcification of the valve leaflets is among the leading causes of aortic valve disease in the elderly and is the most frequent reason for prosthetic valve replacement in adults [1]. Over the past fifty years there have been significant advances in the development of prosthetic aortic replacement valves; however, several challenges still remain due to their poor long-term durability caused by calcification and mechanical failure [2]. Further research is needed to improve their longevity and to advance our understanding of their operation. The in vitro characterization of a valve prosthesis is a key part of the valve development process since it provides useful insight into the functioning of the prosthesis under physiologically normal conditions. It also provides detailed information for initialization and validation of fluid dynamic and finite element simulations of prosthetic valves. Many nonintrusive techniques, including cineradiography [3], Doppler echocardiography [4-6], qualitative flow visualization [3,7-8], laser Doppler velocimetry [9-10], magnetic resonance image velocity mapping [11-12], particle image velocimetry [13-14] and phonocardiography [15] have been previously used to characterize native and prosthetic valves.

The aim of this paper is to characterize a prototype 19mm diameter bioprosthetic valve using Doppler echocardiography and qualitative flow visualization.

II. EXPERIMENTAL SETUP

A. Valve Model

The prototype aortic valve tested in this study is intended for transcatheter insertion and deployment via balloon expansion in the native aortic position. The valve is supported on a 19 mm diameter (inner), electro-polished, L-605 cobalt-chrome stent. The leaflets of the valve were made from kangaroo pericardium treated with the ADAPT® anti-calcification process and were attached to the stent with CV-7 Gore-Tex© polytetrafluoroethylene suturing, as shown in Fig. 1 (a). Paravalvular leakage was prevented by enclosing the stent inside a 0.25 mm thick, biocompatible BARD polyester knit tube. The fiber alignment of the leaflet tissue was chosen to be in line with the circumferential direction of the valve to improve its strength. Since one side of the tissue was smooth while the other was fibrous, the smooth side was used for sealing between the leaflets, while the fibrous side was used for the inner part of the leaflet which comes into direct contact with the stent during valve operation. Full details of the prosthetic valve fabrication process are reported by Smuts [16]. Also, prior to fabrication the mechanical and physical properties of the leaflet tissue were characterized by biaxial testing and histological analysis (Table I). A 21 mm (inner) diameter St. Jude Medical Epic™ porcine tricuspid valve, shown in Fig. 1 (b), was used as a control.

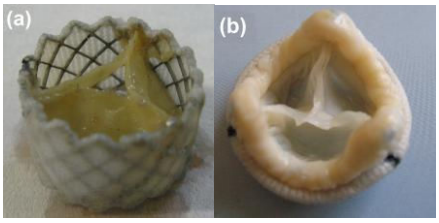

Fig.1. (a) Prototype 19mm diameter prosthetic aortic valve with kangaroo tissue leaflets and (b) Control valve (21 mm diameter St. Jude Medical Epic™ porcine tricuspid valve).

TABLE I
PROTOTYPE VALVE DIMENSIONS AND PROPERTIES

Property	Value	Units
Valve diameter (inner)	19.0	mm
Stent height	16.0	mm
Average leaflet height	14.0	mm
Leaflet thickness	0.19–0.29	mm
Avg. leaflet free edge length	21.6	mm
Maximum normal leaflet stress	9.09×10^5	Nm^{-2}
Maximum leaflet strain	0.32	—

B. Experimental Setup

The valves were mounted in a custom-built cardiac pulse duplicator (CPD) system which simulates the pumping action of the left ventricle of the heart. The design of the system was based on the 4-element Windkessel model of the arterial system which uses a simple lumped parameter electrical analogy to simulate the total arterial impedance in the human body. The influence of anatomical features of the

Manuscript received March, 2012.

Cornie Scheffer, Kiran Dellimore, Iain Kemp and Reynaldo Rodriguez are with the Biomedical Engineering Research Group, Department of Mechanical and Mechatronic Engineering, Stellenbosch University, South Africa (phone: +27218084249; fax: +27218084958; e-mail: cscheffer@sun.ac.za).

aorta on the flow waveforms was accounted for by varying the flow compliance, inertance and resistance. The CPD has four separate valve chambers for testing valve prostheses at heart rates up to 250 bpm and is controlled via a LabView® graphical user interface. The working fluid in the CPD is a mixture of 48% glycerol and 52% saline solution (by mass), with 0.01% sodium azide disinfectant, which has a similar density (1.05×10^3 kgm^{-3}) and viscosity (3.57×10^{-3} Ns•m^{-2}) to whole blood with a physiological hematocrit of 45% at 37 ^{0}C. A glycerol based blood analog was used, since work by Carey et al. [17] has shown that glycerol absorption does not adversely affect leaflet stiffness or mechanical performance and because similar blood analogs have been used in several previous studies [3,13-14]. The mixture was heated using two submersible RS Components 300 W heaters with a network of five HT model HJ-541 pumps to ensure that the mixture was at a uniform temperature. The mixture temperature was maintained at 37 ^{0}C using a Delta DTA PID controller with a RTD PT100 sensor which regulated the temperature to within 0.2 ^{0}C.

The valve characterization experiments were performed at a heart rate of 72 bpm which corresponded to a systolic time of 360 ms and a cardiac output of 7.0 L/min. Pressure data were collected upstream and downstream of the valve over several cardiac cycles using two WIKA model A-10 pressure transducers which can measure pressures between 0 to 760 mmHg to within 4 mmHg at a sampling rate of 2 kHz. The compliance of the system was varied by changing the height of the mixture in the compliance chamber and the amount of air trapped in the chamber. The flow resistance was altered by adjusting the orifice area of the pipe to the mixture storage tank using a 50 mm diameter ball valve. To produce a pressure profile within a physiologically normal range it was found that the mixture height in the 90 mm diameter compliance chamber should be set to 603 mm with an air height of 117 mm and an orifice area of less than 10% of the pipe cross-sectional area. Prior to taking all measurements the system was allowed to reach steady state.

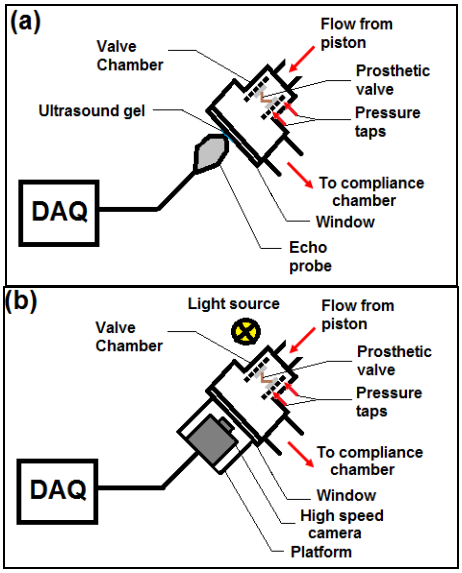

Fig.2. Schematic of the experimental setup for: (a) the Doppler echo measurements and (b) the flow visualization measurements.

C. *Procedure*

Doppler echocardiography was performed with a Sonosite™ MicroMaxx array system using a 25 mm, 1-5 MHz, independent P17 phased array Doppler imaging transducer (probe), capable of operating in continuous and pulsed wave modes. The following parameters were used for all readings: fractional echo readout using 70-100% of the full echo; Doppler angle, 0°; bandwidth, in the range of 5.2-41.7 kHz, velocity sensitivity, 200 cms^{-1} along all 3 spatial directions; fractional field of view, (300-340 x 225-240) mm^2; slab thickness, 83.2-96 mm; matrix, 256 x 144 x 32; and spatial resolution, (1.17-1.33 x 1.56-1.67 x 2.60-3.00) mm^3. The peak flow velocity was measured by placing the probe in-line with the flow through the prosthesis in contact with the window of the valve chamber (Fig. 2a). The Doppler transmit beam was placed as perpendicular as possible to the plane of the valve ring, with very slight angulation of the probe required to obtain the maximal flow velocity. The initial positioning of the sample volume was made with the aid of two-dimensional imaging while the probe was in pulsed Doppler mode. The audio output guided final positioning until an optimal spectral signal was obtained. After the data were obtained in the pulsed mode, the equipment was switched to continuous mode to confirm that the maximal velocities had been recorded. The mean, maximum systolic transvalvular pressure gradient (STVPG) and velocity were measured at different stream-wise locations to characterize the flow before, at and after the valve.

Flow images were acquired using a 0.3 Megapixel Grasshopper GRAS-03K2M-C digital camera at a frame rate of up to 288.2 fps (frames per second) over a period of 5.2 s at a resolution of 152 x 154 pixels. The camera was equipped with a KAI-0340D 1/3 inch image sensor and had a pixel size of 7.4µm x 7.4µm. The pressure transducer measurements were synchronized with the high speed camera image acquisition using a triggering system controlled in LabVIEW. Images were acquired with the camera mounted on a platform attached to the base of the valve chamber with the lens situated 1.1 cm from the valve chamber window and 8.0 cm from the valve (Fig. 2b).

III. Data Analysis

The flow visualization images and pressure transducer measurements were analyzed in MATLAB® (Natick, MA). Noise in the pressure measurements was filtered using a Butterworth low-pass filter. The rapid valve opening time (RVOT) was calculated from the camera images based on the time taken for the valve to go from a closed to an open position. The rapid valve closing time (RVCT) was computed from the time when the valve started to close until it was completely closed. The ejection time (ET) was found by computing the time taken from the initial opening to complete closure of the valve. All values for RVOT, RVCT and ET were obtained by averaging over several cardiac cycles and are reported as mean ± S.D in Table II. The cardiac output, Q, was calculated by multiplying the stroke volume by the heart rate. The peak systolic velocity was computed from the Doppler sonograms as the highest value of the velocity

time integral during systole. The peak STVPG was obtained in two ways. It was read as an output from the Doppler sonograms and it was computed from the pressure transducer measurements by finding the difference between the aortic and ventricular pressures.

IV. Results

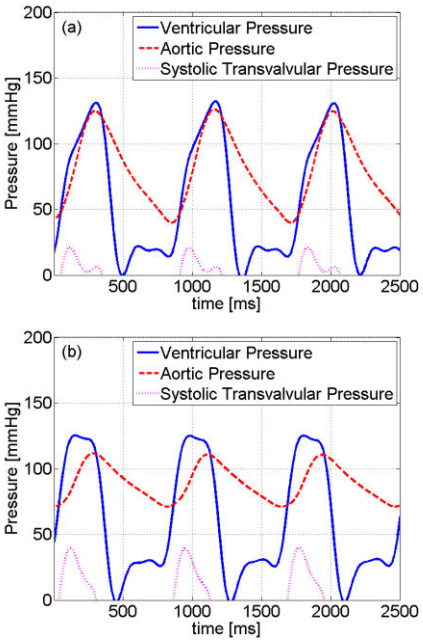

Fig.3. Time variation of aortic (dashed line), ventricular (solid line) and systolic transvalvular (dotted line) pressure for the flow through: (a) the prototype 19mm valve and (b) the control valve.

Fig. 3 (a) and (b) show the time variation of the pressure waveforms of the flow in the prototype prosthetic valve and the control valve at 72 bpm. The solid line corresponds to the ventricular pressure, the dashed line to aortic pressure and the dotted line to the transvalvular pressure gradient. For the prototype valve the peak systolic aortic pressure was 131.2 mmHg and the minimum diastolic pressure was 40.0 mmHg. For the control valve the peak systolic aortic pressure and the minimum diastolic pressure were 125.4 mmHg and 71.1 mmHg, respectively.

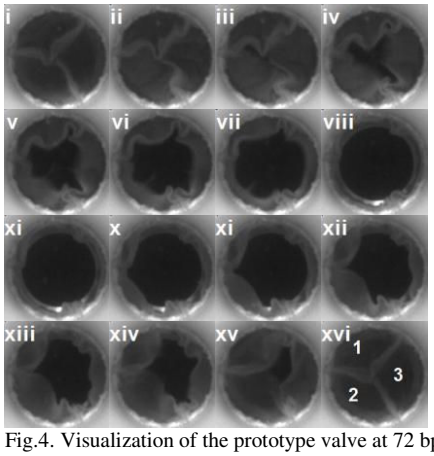

Fig.4. Visualization of the prototype valve at 72 bpm.

Fig. 4 and 5 present still images showing the opening (images i-viii) and closing (images ix-xvi) of the prosthetic and control valves at 72 bpm. For the prosthetic valve in Fig. 4, the RVOT was 31 ms while the RVCT was 100 ms and ET was 360 ms. For the control valve in Fig. 5, the RVOT was 50 ms while the RVCT was 120 ms and the ET was 350 ms.

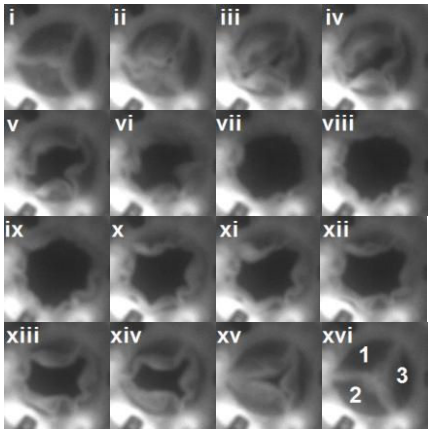

Fig.5. Visualization of the control valve at 72 bpm.

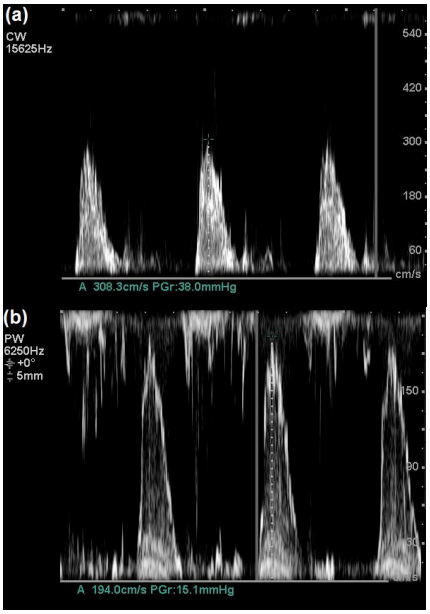

Fig.6. Doppler sonograms of the prototype valve at 72 bpm.

Fig. 6 shows continuous and pulsed wave Doppler echo sonograms of the prototype valve in operation at 72 bpm. The peak systolic velocity and STVPG measured using the echo probe were 308.3 cm/s and 38.0 mmHg, respectively.

TABLE II
SUMMARY OF THE VALVE OPENING AND CLOSING DYNAMICS

Valve	RVOT (ms)	RVCT (ms)	ET (ms)	STVPG (mmHg)
Prototype	42.9±3.5	86.7±22.0	360.5±3.6	20.7±0.3
Control	50.8±1.4	120.8±5.5	349.2±12.4	39.5±0.3

V. Discussion

The results shown in Fig. 3 (a)-(b) suggest that a close to physiologically normal environment was produced for the prosthetic and control valve tests. The ratios of systolic to diastolic aortic pressure for the prototype and control valves were 131/40 and 125/71 respectively which indicates that the peak systolic pressures were pre-hypertensive while the

minimum diastolic pressures were normal and hypotensive for the control and prototype valves, respectively.

Comparison of the high-speed camera images shown in Fig. 4 i-xvi reveal several key insights into the dynamics of the prototype valve at 72 bpm. During opening of the valve (Fig. 4 i-xviii), the leaflets are observed to initially spread apart gradually before undergoing a period of rapid separation in which the valve transitions from being open by a narrow slit to fully open. The separation of the leaflets is also fairly uniform which results in a symmetric valve opening. However, the valve dynamics are significantly different during closing (Fig. 4 ix-xvi), with leaflets 1 and 2 approaching each other at a faster rate than leaflet 3. This asymmetry in closing is likely due to the high STVPG (20.7 mmHg) and may indicate that leaflet 3 is experiencing a heavier stress load than the other leaflets. The increased loading of leaflet 3 could lead to long term leaflet damage (e.g., tearing) and loss of valve function. Similar trends are observed for the dynamics of the control valve shown in Fig. 5 i-xvi. The opening of the valve leaflets is relatively symmetric as was observed for the prototype valve, while closing is highly asymmetric, with leaflets 1 and 2 close more rapidly than leaflet 3. The asymmetry in closing is likely due to the large STVPG across the control valve (39.5 mmHg). The RVOT and ET for the prototype and control valves were comparable, while the RVCT was significantly longer for the control valve due to its larger STVPG.

The Doppler image shown in Fig. 6 (a) indicates that the peak systolic velocity through the prototype valve, which occurs at the leaflets, was 308.3 cm/s. This fairly large value at a heart rate of just 72 bpm can be attributed to two main factors. First, the diameter of the prototype valve (19 mm) is smaller than that of a typical native human aortic valve (about 23 mm) which means that for the same cardiac output the average velocity of the flow will be 46.5% higher, based on mass conservation. Second, the cardiac output was 7.0 L/min, which is slightly higher than in normal human adults (5.0-6.0 L/min). Fig. 6 (b) shows a Doppler sonogram of the flow on the ventricular side of the prototype valve. The peak systolic velocity and pressure gradient at this location were 194.0 m/s and 15.1 mmHg, respectively, which represents a 37.1% drop in velocity and a 60.3% drop in the pressure gradient relative to the conditions at the valve leaflets. This suggests that the flow rapidly accelerates as it passes through the leaflets from the ventricular to aortic side of the valve.

VI. Conclusion

The performance of a 19 mm diameter prototype bioprosthetic aortic valve was characterized using Doppler echocardiography and qualitative flow visualization at a heart rate of 72 bpm. Analysis of the flow visualization images revealed that the prototype and control valve leaflets open symmetrically but close asymmetrically. The asymmetry in the closing of the valves is likely due to the large pressure gradients across the valves and may have implications for the long term mechanical failure of the valves. The relatively high peak systolic velocity of 309.9 cm/s, which was measured in the prototype valve, can be attributed to the small valve diameter and the high cardiac output used in the current study.

VII. Future work

Future work will explore the characterization of 23 mm diameter prototype valves and long term fatigue testing.

Acknowledgment

The authors are grateful to Dr. Renier Verbeek for his help with the echocardiographic measurements. The support of Celxcel Pty Ltd., Perth, Australia, in providing tissue for the valves is also greatly appreciated.

References

[1] F. A. Flachskampf, W. G. Daniel, "Aortic valve stenosis," *Internist (Berl)*, vol. 45 no.11, pp.1281–1290, 2004.

[2] W. Lim, Y. Chew, T. Chew, H. Low, "Steady flow velocity field and turbulent stress mappings downstream of a porcine bioprosthetic aortic valve in vitro," *Annals of Biomedical Engineering*, vol. 25, pp.86−95, 1997.

[3] V. Bjork, A. Henze, T. Hindmarsh, "Radiopaque marker in the tilting disc of the Björk-Shiley heart valve: evaluation of in vitro prosthetic function by cineradiography," *Journal of Thoracic Cardiovascular Surgery*, vol. 73, pp.563–569, 1977.

[4] J. Douglas, D. Williams, "Echocardiographic evaluation of the Björk-Shiley prosthetic valve," *Circulation*, vol. 50, pp.52–57, 1974.

[5] R. Leyh, C. Schmidke, H. Sievers, M. Yacoub, "Opening and closing characteristics of the aortic valve after different types of valve-preserving surgery," *Circulation*, vol.100, pp.2153–60, 1999.

[6] T. Aybek, M. Sotiriou, T. Wöhleke, A. Miskovic, A. Simon, M. Doss, S. Dogan, G. Wimmer-Greinecker, A. Moritz, "Valve opening and closing dynamics after different aortic valve-sparing operations," *Journal of Heart Valve Disease*,vol.14, pp.114–120, 2005.

[7] C. Yap, H. Kim, K. Balachandran, M. Weiler, R. Haj-Ali, A. Yoganathan, "Dynamic deformation characteristics of porcine aortic valve leaflet under normal and hypertensive conditions," *American Journal of Physiology Heart and Circulatory Physiology*, vol.298, pp.H395–H405, 2010.

[8] P. Haaf, M. Steiner, T. Attmann, G. Pfister, J. Cremer, G. Lutter, "A novel pulse duplicator system: Evaluation of different valve prostheses," *Thoracic Cardiovascular Surgery*, vol.57 no.1, pp.10−17, 2009.

[9] B. Khalighi, K. Chandran, C. Chen, "Steady flow development past valve prostheses in a model human aorta. I. Centrally occluding valves," *Journal of Biomechanics*, vol.16, pp.1003–1011, 1983.

[10] K. Chandran, G. Cabell, B. Khalighi B, C. Chen, "Pulsatile flow past aortic valve bioprostheses in a model human aorta," *Journal of Biomechanics*, vol.17, pp.609–619, 1984.

[11] J. Kvitting, T. Ebbers, L. Wigstrom, J. Engvall, C. Olin, A. Bolger, "Flow patterns in the aortic root and the aorta studied with time-resolved, three-dimensional, phase-contrast magnetic resonance imaging: implications for aortic valve-sparing surgery," *Journal of Thoracic Cardiovascular Surgery*, vol.127, pp.1602–1607, 2004.

[12] A. Ranga, O. Bouchot, R. Mongrain, P. Ugolini, R. Cartier, "Computational simulations of the aortic valve validated by imaging data: Evaluation of valve-sparing techniques," *Interactive Cardiovascular and Thoracic Surgery*, vol.5, pp.373–378, 2006.

[13] M. Marassi, P. Castelini, M. Pinotti, L. Scalise, "Cardiac valve prosthesis flow performances measured by 2D and 3D-stereo particle image velocimetry," *Experiments in Fluids*,vol.36, pp.176–186, 2004.

[14] R. Kaminsky, S. Kallweit, M. Rossi, U. Morbiducci, L. Scalise, P. Verdonck, E. Tomasini, "PIV measurements of prosthetic heart valve dynamics," *Topics in Applied Physics*, vol.112, pp.55–72, 2008.

[15] B. R. Brodie, W. Grossman, L. P. McLaurin, P. J. Starek, E. Craige, "Diagnosis of prosthetic mitral valve malfunction with combined echo-phonocardiography," *Circulation*, vol. 53, pp.93–100, 1976.

[16] A. N. Smuts, "*Design of tissue leaflets for a percutaneous aortic valve,"* M.Sc. thesis, University of Stellenbosch, 2009.

[17] R. F. Carey, B. A. Herman, "The effects of a glycerin-based blood analog on the testing of bioprosthetic heart valves," *Journal of Biomechanics*, vol. 22, pp.1185−1192, 1989.